Biochem. J. (2010) **430**, 161–169 (Printed in Great Britain) doi:10.1042/BJ20100082

The myeloperoxidase-derived oxidant HOSCN inhibits protein tyrosine phosphatases and modulates cell signalling via the mitogen-activated protein kinase (MAPK) pathway in macrophages

Amanda E. LANE*, Joanne T. M. TAN*, Clare L. HAWKINS*, Alison K. HEATHER*† and Michael J. DAVIES*‡[1]

*The Heart Research Institute, 7 Eliza Street, Newtown, Sydney, NSW 2042, Australia, †Department of Medical and Molecular Biosciences, University of Technology, Sydney, Broadway, NSW 2007, Australia, and ‡Faculty of Medicine, University of Sydney, Sydney, NSW 2006, Australia

MPO (myeloperoxidase) catalyses the oxidation of chloride, bromide and thiocyanate by hydrogen peroxide to HOCl (hypochlorous acid), HOBr (hypobromous acid) and HOSCN (hypothiocyanous acid) respectively. Specificity constants indicate that SCN^- is a major substrate for MPO. HOSCN is also a major oxidant generated by other peroxidases including salivary, gastric and eosinophil peroxidases. While HOCl and HOBr are powerful oxidizing agents, HOSCN is a less reactive, but more specific, oxidant which targets thiols and especially low pK_a species. In the present study we show that HOSCN targets cysteine residues present in PTPs (protein tyrosine phosphatases) with this resulting in a loss of PTP activity for the isolated enzyme, in cell lysates and intact J774A.1 macrophage-like cells. Inhibition also occurs with MPO-generated HOCl and HOBr, but is more marked with MPO-generated HOSCN, particularly at longer incubation times. This inhibition is reversed by dithiothreitol, particularly at early time points, consistent with the reversible oxidation of the active site cysteine residue to give either a cysteine–SCN adduct or a sulfenic acid. Inhibition of PTP activity is associated with increased phosphorylation of p38a and ERK2 (extracellular-signal-regulated kinase 2) as detected by Western blot analysis and phosphoprotein arrays, and results in altered MAPK (mitogen-activated protein kinase) signalling. These data indicate that the highly selective targeting of some protein thiols by HOSCN can result in perturbation of cellular phosphorylation and altered cell signalling. These changes occur with (patho)physiological concentrations of SCN^- ions, and implicate HOSCN as an important mediator of inflammation-induced oxidative damage, particularly in smokers who have elevated plasma levels of SCN^-.

Key words: cell signalling, hypothiocyanous acid (HOSCN), mitogen-activated protein kinase (MAPK), myeloperoxidase, p38, protein tyrosine phosphatase, thiol.

INTRODUCTION

MPO (myeloperoxidase) is a highly basic haem enzyme that is released extracellularly by activated neutrophils, monocytes and some macrophages. MPO catalyses the oxidation of halide (Cl^-, Br^-) and pseudohalide (thiocyanate ion, SCN^-) ions by H_2O_2 (hydrogen peroxide) to the corresponding hypohalous acids: HOCl (hypochlorous acid), HOBr (hypobromous acid) and HOSCN (hypothiocyanous acid; cyanosulfenic acid) (reviewed in [1–3]). These species exist as a mixture of their acid and anion forms at physiological pH values (pK_a 7.6, 8.7 and approx. 5.3 respectively; reviewed in [1]); HOCl, HOBr and HOSCN are used hereon to indicate the physiological mixtures of these species. Cl^- is present at much higher concentrations in plasma (100–140 mM) than other anions with which MPO reacts (Br^-, 20–100 μM; SCN^-, 20–250 μM; [4,5]), but MPO has a much greater specificity constant for SCN^- than for Cl^- or Br^- (approx. 730- and 60-fold greater respectively; [5]). This results in a significant proportion of the H_2O_2 consumed by MPO being utilized to oxidize SCN^- at pH 7.4, and HOSCN is a major oxidant generated by MPO in plasma [5,6]. Other peroxidases, including salivary-, gastric- and eosinophil-peroxidase, also have high specificity constants for SCN^-, resulting in significant yields of HOSCN (reviewed in [1,6]). This is of particular importance in saliva, stomach lining fluid and the airway lining fluid, where SCN^- is concentrated [7,8]. Formation of HOSCN may also be of particular significance in smokers who have markedly elevated plasma SCN^- concentrations [9]. HOCl and HOBr also react rapidly with SCN^-, thereby enhancing the yield of HOSCN [10,11]. HOSCN is therefore a major oxidant generated both directly by multiple peroxidases at sites of inflammation, and as a result of secondary reactions [6].

HOCl and HOBr are powerful oxidants and important components of the human immune response against invading pathogens [2]. However, excessive or misplaced production of these species can result in host tissue damage, with this having been implicated in a wide range of human inflammatory diseases, including cardiovascular disease, rheumatoid arthritis, asthma, cystic fibrosis, some cancers, certain neurodegenerative conditions, kidney disease and inflammatory bowel disease (reviewed in [1–3,12]).

In contrast with HOCl and HOBr which react rapidly with multiple cellular and extracellular targets (reviewed in [13]), HOSCN is highly selective, with the reaction occurring predominantly with thiol (RSH) groups [14], with rate constants, k, in the range 10^4–10^6 $M^{-1} \cdot s^{-1}$ [15,16]. Reaction with tryptophan residues may also be significant when thiol residues are absent or depleted [17]. This selective targeting of thiols has been shown to result in a more marked induction of apoptosis by HOSCN, than equimolar concentrations of HOCl and HOBr, with some cells ([18]; reviewed in [6]).

Abbreviations used: DTT, dithiothreitol; ECL, enhanced chemiluminescence; ERK, extracellular-signal-regulated kinase; HOBr, hypobromous acid; HOCl, hypochlorous acid; HOSCN, hypothiocyanous acid; HRP, horseradish peroxidase; LPO, lactoperoxidase; MAPK, mitogen-activated protein kinase; MKK, MAPK kinase; MPO, myeloperoxidase; PTP, protein tyrosine phosphatase.

[1] To whom correspondence should be addressed (email daviesm@hri.org.au).

The potential role of HOSCN in human disease is poorly understood, but previous studies have provided evidence for a role for SCN^--derived species in models of atherosclerosis, and humans with cardiovascular disease [9,19–21]. These data are of particular relevance to smokers who typically have elevated levels of SCN^- and an increased risk of multiple pathologies.

Phosphorylation of tyrosine, threonine and serine residues plays a key role in the regulation of signal transduction in mammalian cells, and hence control of cell activation, cell-cycle progression, cytoskeletal rearrangement, cell movement, differentiation, apoptosis and metabolic homoeostasis [22,23]. Phosphorylation is typically reversible and dynamic with the extent governed by the opposing activities of large families of protein tyrosine kinases and PTPs (protein tyrosine phosphatases) in the case of tyrosine phosphorylation [24]. Oxidants can modulate signalling by both enzyme families, as both PTPs and kinases are redox sensitive [25]. Oxidation of PTP cysteine residues, and particularly the low pK_a active site cysteine, occurs with multiple oxidants including H_2O_2 [26], peroxynitrite [27], singlet oxygen [28] and amino acid and protein peroxides [29], with this resulting in enzyme inactivation. In contrast, oxidation of kinases can result in activation, either by cysteine modification or other mechanisms [25,30]. Such perturbations have been implicated in a number of diseases including cancer, diabetes, rheumatoid arthritis and hypertension [22,24,25]. One member of this family, PTP1B is an important enzyme in the negative regulation of the insulin receptor and a therapeutic target in Type 2 diabetes and obesity [31]. The active site cysteine residue [32] can be reversibly oxidized to a sulfenyl-amide species, which causes large changes in the PTP1B active site; this can be reversed by the key cellular reducing agent glutathione, although it can also undergo irreversible oxidation to higher oxy acids [31].

In light of the selectivity of HOSCN for thiol residues, and particularly low pK_a species [15], and evidence for the induction of apoptosis by HOSCN [6,18], we hypothesized that PTPs might be cellular targets of HOSCN, and that this might result in altered cellular signalling. We demonstrate in the present study that HOSCN inhibits isolated PTP1B, and PTP activity in J774A.1 cells. The inhibition occurs at pathophysiological concentrations of oxidant. This loss of activity is accompanied by hyperphosphorylation of p38α and ERK2 [extracellular-signal-regulated kinase 2; MAPK1 (mitogen-activated protein kinase 1)] and increased expression of transcription factors, suggesting that HOSCN induces apoptosis via the MAPK pathway in macrophages.

EXPERIMENTAL

Materials

Aqueous solutions and buffers were prepared using nanopure water filtered through a four-stage Milli-Q system (Millipore Waters). LPO (lactoperoxidase; from bovine milk; Calbiochem) was quantified by absorbance at 412 nm using a molar absorption coefficient of 112000 $M^{-1} \cdot cm^{-1}$ [33]. H_2O_2 [30 % (v/v) solution; Merck] was quantified at 240 nm using a molar absorption coefficient of 39.4 $M^{-1} \cdot cm^{-1}$ [34]. Antibodies were obtained from the following sources: anti-human/mouse/rat ERK1/ERK2 monoclonal antibody, anti-phospho-ERK1 (Thr^{202}/Tyr^{204})/ERK2 (Thr^{185}/Tyr^{187}) monoclonal antibody, anti-human/mouse/rat p38α monoclonal antibody, anti-phospho-p38 MAPK affinity-purified antibody, anti-human/mouse/rat MKK (MAPK kinase) 3/MKK6 monoclonal antibody (all R&D Systems), anti-phospho-MKK3/6 monoclonal antibody (Cell Signalling Technology) and β-actin antibody (Santa Cruz Biotechnology). Secondary antibodies were: sheep anti-mouse Ig, peroxidase-conjugated (Chemicon, Millipore) and ECL (enhanced chemiluminescence) rabbit IgG, HRP (horseradish peroxidase)-linked whole antibody (from donkey) (GE Healthcare).

Cell culture

Murine macrophage-like J774A.1 cells (A.T.C.C.) were cultured under sterile conditions in DMEM (Dulbecco's modified Eagle's medium; Sigma–Aldrich) supplemented with 10 % (v/v) heat-inactivated fetal bovine serum (Invitrogen), 2 mM L-glutamine (Thermotrace), 100 units/ml penicillin and 0.1 mg/ml streptomycin (Invitrogen). Cells were seeded at 0.5×10^6 cells/ml in six-well plates. The medium was removed and cells washed twice with PBS (Amresco) before treatment. Protein concentrations were determined using the BCA (bicinchoninic acid) assay (Pierce) using BSA standards (Sigma).

Preparation of HOSCN

HOSCN was prepared enzymatically by incubation of LPO (1.5–2 mM) for 15 min with NaSCN (7.5 mM; Sigma) and H_2O_2 (3.75 mM added as 5×10 μl aliquots, 1 min apart) in 10 mM potassium phosphate buffer (pH 6.6; Sigma) at 22 °C. The reaction was stopped by the addition of catalase (140 i.u., bovine liver; Sigma), with this enzyme and LPO subsequently removed by centrifugation through a 10000 Da molecular-mass cut-off filter (Pall Life Sciences) at 11 200 ***g*** for 5 min. HOSCN was quantified by reaction with TNB (5-thio-2-nitrobenzoic acid; Sigma), with a molar absorption coefficient of 14150 $M^{-1} \cdot cm^{-1}$ at 412 nm [17,18], and used immediately.

PTP activity assay

PTP activity was determined by quantifying the conversion of *p*-nitrophenyl phosphate (Calbiochem) into the *p*-nitrophenolate anion as described previously [29], with the latter quantified by A_{405} and comparison with a *p*-nitrophenolate standard curve (Sigma). PTP activity was determined after exposure of isolated PTP1B (recombinant protein from *Escherichia coli*; Calbiochem) or J774A.1 cell lysates (0.33 ± 0.03 mg of protein/ml) to HOSCN, enzyme reactions or control treatments for the times stated. For the isolated PTP1B studies, DTT (dithiothreitol) present in the commercial preparations was removed before use by washing the enzyme with buffer using a 3000 Da molecular-mass cut-off filter spun at 11 200 ***g***. The enzyme (0.5 μM, 18.7 $\mu g \cdot ml^{-1}$) was subsequently exposed to phosphate buffer or HOSCN for 5 min at 22 °C. Then, 10 ml of 2.5 mM cysteine (to quench the remaining HOSCN) was added to 70 μl aliquots of the reaction mixture in a 96-well plate, then 10 μl of 4 mM *p*-nitrophenyl phosphate was added and incubated for 60 min at 22 °C. The reaction was subsequently stopped by the addition of 10 μl of 0.1 M KOH and the absorbance at 405 nm was recorded.

Intact J774A.1 cells were exposed to HOSCN at the concentrations indicated, in PBS, and incubated for the times indicated at 22 °C. Any residual oxidant was removed by aspiration of the cell supernatant, with the remaining cells carefully scraped into PBS (0.5×10^6 cells/ml) and centrifuged at 1000 ***g*** for 5 min. The cells were resuspended at 4×10^6 cells/ml, and treated with nanopure water and freeze–thawed on dry ice to ensure lysis. The PTP assay was performed using 0.32 ± 0.06 mg of protein/ml. Incubation of cell lysates with MPO-generated oxidants was carried out by incubation of the lysates (as above) with MPO (100 nM) and H_2O_2 (25 μM added as

5×2.8 μl aliquots, 1 min apart) in the presence of 100 μM Cl^- or 100 μM Br^- or various concentrations of SCN^- at pH 7.4 at 22 °C in 10 mM potassium phosphate buffer. MPO was removed after reaction with *p*-nitrophenyl phosphate and prior to quantification of the *p*-nitrophenolate anion by centrifugation of the solution through a 10000 Da molecular-mass cut-off filter (Pall Life Sciences) at 11 200 ***g*** for 5 min.

Quantification of thiols

ThioGlo-1™ (Calbiochem) was used for the fluorometric quantification of thiols [35]. Stock solutions of ThioGlo™ (2.6 mM) in acetonitrile were prepared and stored at 4 °C. Immediately prior to use, the stock was diluted 1:100 in PBS (pH 7.5). Working reagent (50 μl) was added to 50 μl of the isolated PTP1B and incubated for 5 min at 22 °C. Thiol concentrations were quantified by fluorescence spectroscopy with $\lambda_{ex} = 360$ nm and $\lambda_{em} = 530$ nm using GSH (Sigma–Aldrich) to construct a standard curve. The absolute levels of thiols detected on the isolated PTP1B was less than expected based on the protein composition (compare with UniProtKB/Swiss-Prot accession number P18031), indicating that some oxidation of the enzyme had occurred during isolation/handling.

Phospho-MAPK antibody array

The MAPK signalling pathway was investigated using a Proteome Profiler™ Human Phospho-MAPK Antibody Array following the manufacturer's protocol (R&D Systems). J774A.1 cells (1×10^6) were exposed to 50 μM HOSCN for 15 min, then cell proteins were extracted and the concentration determined (Lowry assay, Bio-Rad). Total cell protein (300 μg) was hybridized to the array membranes, the arrays were washed and incubated with the detection antibody cocktail labelled with streptavidin–HRP. Chemiluminescent detection was performed with ECL (Amersham). Signals were directly digitized using a ChemiDoc XRS (Bio-Rad).

Western blot analysis

Cells (1×10^6 cells/ml) were treated with HOSCN (15 min at 22 °C), total protein was extracted with RIPA buffer [50 mM Tris/HCl (pH 8), 150 mM NaCl, 1 % Nonidet P40, 0.1 % SDS, 0.5 % sodium deoxycholate and 1:100 diluted proteinase inhibitor cocktail] and protein was quantified using the Lowry assay (Bio-Rad). Protein (20–35 μg) was separated by SDS/PAGE on 12 % acrylamide gels, then transferred on to nitrocellulose membranes (iBlot™, Invitrogen). The membrane was then probed with either anti-ERK1/2 antibody (1:1000), anti-phospho-ERK1/2 antibody (1:1000), anti-p38α antibody (1:1000), anti-phospho-p38 antibody (1:2000), anti-MKK3/6 antibody (1:500) or anti-phospho-MKK3/6 antibody (1:1000). After a wash step, a secondary antibody was applied which was either peroxidase-conjugated sheep anti-mouse Ig or donkey anti-rabbit IgG (1:2000). The secondary antibodies were subsequently detected by ECL as described above. Band densities were quantified using Quantity One software (Bio-Rad) and normalized to the levels of β-actin, the housekeeping control protein. β-Actin levels were measured after stripping the membranes [200 mM glycine, 1 % (w/v) SDS and 1 % (v/v) Tween 20 (pH 2.2)] and subsequent re-probing with β-actin antibody (1:2000).

MAPK signalling pathway PCR array

Cells were treated with 0 (buffer) or 50 μM HOSCN for 15 min at 22 °C, and then total RNA was extracted using the RNeasy Plus Mini Kit (Qiagen). Each well was extracted individually and, following isolation, two wells were pooled and concentrated to half the original volume using a vacuum concentrator (Vacufuge Concentrator 5301; Eppendorf). The SYBR-Green II RNA assay (Molecular Probes, Invitrogen) was used to normalize all samples to a concentration of 200 ng/ml. The integrity of the RNA was verified using an Experion bioanalyser (Bio-Rad). The mRNA within each sample was converted into cDNA using a reverse transcription RT^2 First Strand Kit (SA Biosciences). The resultant cDNA was assayed by PCR amplification using a MAPK Signalling Pathway PCR Array kit (SA Biosciences) based on the RT^2 SYBR green/Fluorescein PCR master mix (SA Biosciences). PCR amplification was performed using an iCycler (Bio-Rad). Analysis of gene expression was completed using SA Biosciences PCR Array Data Analysis Web Portal, as recommended by the manufacturers, and verified using the $\Delta\Delta C_t$ method.

Statistical analyses

Statistical analysis was performed using GraphPad Prism software 4.0 (GraphPad Software, http://www.graphpad.com) using one- or two-way ANOVA with Bonferroni's or Tukey's post-hoc test (as indicated) with $P < 0.05$ taken as statistically significant.

RESULTS

Inhibition of isolated PTP1B activity by HOSCN

Isolated PTP1B (0.5 μM) was incubated with 0–25 μM HOSCN (generated enzymatically using a LPO/H_2O_2/SCN^- system; see the Experimental section) for 5 min at 22 °C (pH 7.4), before assessment of the remaining enzyme activity using the conversion of *p*-nitrophenyl phosphate into *p*-nitrophenolate anion, with the latter quantified spectrophotometrically at 405 nm. Exposure to HOSCN resulted in a significant concentration-dependent decrease in activity relative to control samples at concentrations of HOSCN $\geqslant$12.5 μM (i.e. $\geqslant$25-fold molar excess of oxidant relative to protein; Figure 1A). The loss of activity was time-dependent, with 5 μM HOSCN (10-fold molar excess of oxidant) inducing $\sim$90 % inhibition by 120 min (results not shown). A slow loss of activity was also detected in control incubations with buffer alone over extended incubation times, presumably due to thiol autoxidation ($\sim$37 % inhibition by 120 min; results not shown).

The role of cysteine modification in this inhibition was examined by quantifying protein thiol levels in identical incubations using ThioGlo-1™, which reacts with free thiols to give fluorescent adducts. Treatment of PTP1B with oxidant resulted in a significant decrease in protein thiol concentration, with this being significant at $\geqslant$2.5 μM HOSCN (i.e. >5-fold molar excess of oxidant to protein; Figure 1B). No significant background fluorescence was detected in control experiments performed in the absence of PTP1B indicating that HOSCN does not react directly with ThioGlo-1™.

Inhibition of PTP activity in cell lysates and intact cells by HOSCN

Incubation of J774A.1 cell lysates with 0–200 μM HOSCN for 5 min resulted in a concentration-dependent loss of PTP activity. This loss of activity was statistically significant with $\geqslant$10 μM HOSCN when compared with controls treated with phosphate buffer alone (Figure 2A). This loss of activity was time-dependent,

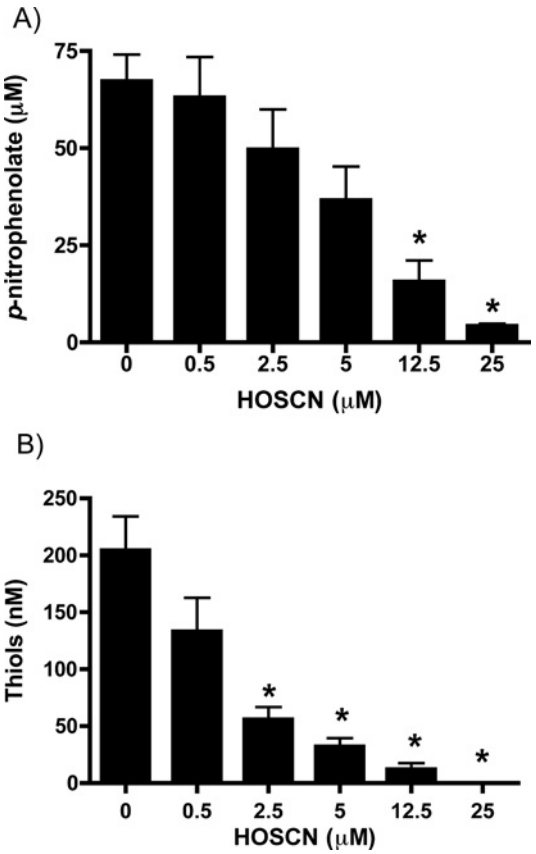

Figure 1 Inhibition of isolated PTP1B activity and loss of cysteine residues on treatment with HOSCN

Isolated PTP1B was washed with buffer using a 3000 Da molecular mass cut-off filter to remove DTT present in the commercial preparation before use. The protein (0.5 μM, 18.7 $\mu g \cdot ml^{-1}$) was subsequently exposed to HOSCN at the concentrations indicated for 5 min at 22 °C before determination of residual enzymatic activity and remaining thiols. (**A**) PTP activity (0.090 μM, 3.3 $\mu g \cdot ml^{-1}$ PTP1B final assay concentration). (**B**) Thiol groups present in isolated PTP1B (0.25 μM, 9.35 $\mu g \cdot ml^{-1}$ PTP1B final assay concentration) were measured using ThioGlo-1^{TM} with GSH used to construct a standard curve. Values are means $\pm$ S.E.M. of duplicate determinations from three separate experiments. Statistical analyses compared all concentrations with the 0 μM HOSCN condition using one-way ANOVA with Bonferroni's post-hoc test; $^*P < 0.05$.

with a significantly greater loss of activity detected at 15 min compared with 5 min with 25 μM HOSCN. At longer time points (up to 2 h), no further decrease in activity was detected (Figure 2B). No loss of activity was measured in controls treated with phosphate buffer alone over the same time period.

The potential reversibility of inactivation was examined in lysates treated with 25 μM HOSCN for either 15 or 120 min, with subsequent further incubation with 10 mM DTT for 10 min. For the samples treated with HOSCN for 15 min, DTT treatment induced a partial recovery of activity; however, for those samples exposed to HOSCN for 120 min, the recovery of activity was significantly less (Figure 3). These results suggest that the damage induced by HOSCN is (at least partially) reversible over short time periods, but over longer time periods becomes irreversible.

Treatment of intact J774A.1 cells (5×10^5) with 10–250 μM HOSCN for 60 min in PBS also resulted in a loss of PTP activity, with this becoming significant at oxidant concentrations $\geqslant$100 μM HOSCN (Figure 4). With this concentration of oxidant, significant differences in activity were detected between the control and treated samples at all non-zero time points examined (15, 30 and 60 min; results not shown).

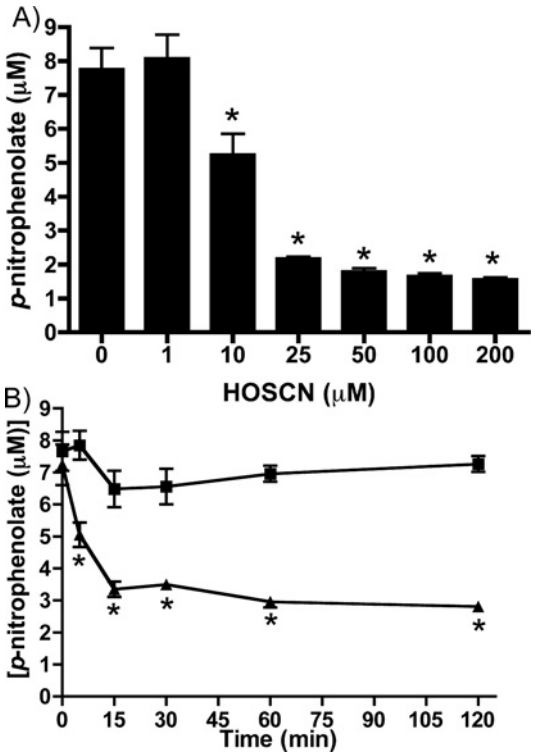

Figure 2 Inhibition of PTP activity in J774A.1 cell lysates by HOSCN

PTP activity in cell lysates (0.33 $\pm$ 0.03 mg of cell protein/ml) was determined after incubation with: (**A**) HOSCN at the concentrations indicated for 5 min; (**B**) phosphate buffer (■) or 25 μM HOSCN (▲) for the times indicated. Values are means $\pm$ S.D. of triplicate determinations from each of four separate experiments. Statistical analyses in (**A**) compared all concentrations with the 0 μM oxidant condition using one-way ANOVA with Bonferroni's post-hoc test; in (**B**) analyses compared the control with HOSCN-treatment at each time point using two-way ANOVA with Bonferroni's post-hoc test. In both cases * indicates $P < 0.05$.

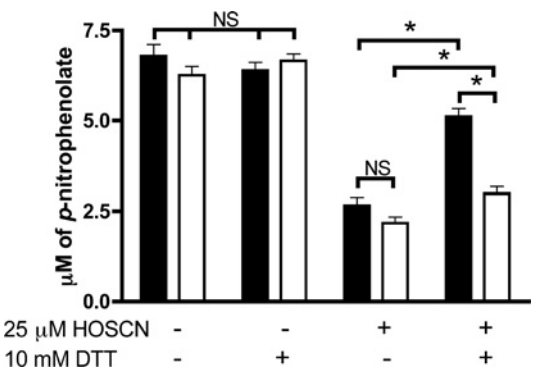

Figure 3 Inhibition of PTP activity in J774A.1 cell lysates by HOSCN is reversible with short exposure times, but irreversible on prolonged oxidant treatment

PTP activity in cell lysates (0.33 $\pm$ 0.03 mg of cell protein/ml) was determined after incubation with phosphate buffer or 25 μM HOSCN for 15 min (solid bars) and 120 min (open bars) at 22 °C followed by treatment with 10 mM DTT for 10 min at 37 °C. Values are means $\pm$ S.E.M. of triplicate determinations from each of four separate experiments. Statistical analyses were carried out using two-way ANOVA with Bonferroni's post-hoc test, $^*P < 0.05$. NS, not significantly different.

Inhibition of PTP activity in cell lysates by MPO-generated oxidants

The above studies were subsequently extended to determine whether oxidants generated by a MPO/H_2O_2/SCN^- system behaved in the same manner to pre-formed HOSCN, and how

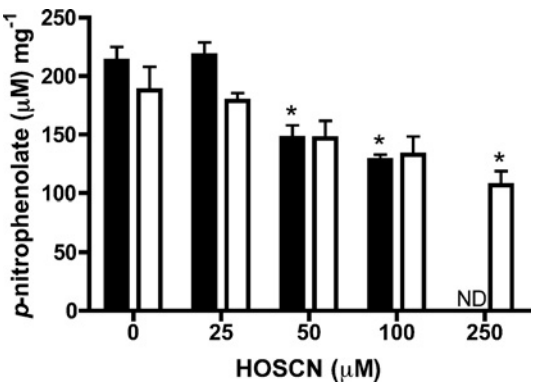

Figure 4 Inhibition of PTP activity in intact J774A.1 cells by HOSCN

PTP activity (expressed per mg of cell protein) in cells (plated at 0.5×10^6 cells/ml with assay performed at 0.32 ± 0.06 mg of cell protein/ml) was determined after incubation with HOSCN, at the concentrations indicated, for either 15 min (solid bars) or 60 min (open bars) at 22 °C. Values are means ± S.E.M. of duplicate determinations from each of two wells from three separate experiments. Statistical analyses compared all concentrations with the 0 μM oxidant conditions using one-way ANOVA with Bonferroni's post-hoc test; $^*P < 0.05$. ND, not determined.

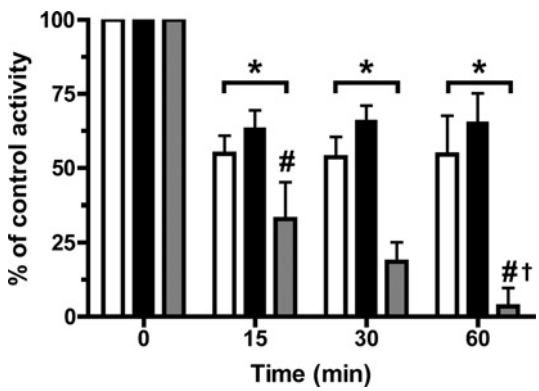

Figure 5 Concentration-dependent inhibition of PTP activity in J774A.1 cell lysates by MPO-derived oxidants

PTP activity in cell lysates (0.33 ± 0.03 mg of cell protein/ml) was determined after incubation with 100 nM MPO and 100 mM Cl^- (open bars), 100 μM Br^- (solid bars) or 100 μM SCN^- (grey bars) with 25 μM H_2O_2 for the times indicated at 22 °C. After incubation the samples were filtered using 10000 Da molecular mass cut-off filters to remove MPO before quantification of the *p*-nitrophenolate anion released from the *p*-nitrophenylphosphate. Controls were incubated in the absence of H_2O_2. Values are means ± S.D. of triplicate determinations from each of three separate experiments. Statistical analyses were carried using two-way ANOVA with Bonferroni's post-hoc test. $^*P < 0.05$ for each of the data sets at each time point compared with the time zero control. $\#P < 0.05$ for the 100 μM SCN^- condition compared with the Cl^- and Br^- conditions at the same time point. $\dagger P < 0.05$ for the 60 min compared with 15 min time points for the 100 μM SCN^- condition.

damage induced by SCN^--derived oxidants might differ from those generated from Cl^- and Br^- at pathophysiological levels.

Incubation of cell lysates (as above) with MPO (100 nM) and H_2O_2 (25 μM, added as five separate aliquots over 5 min) at pH 7.4 in the presence of 100 μM SCN^- resulted in a significant loss of PTP activity after 15 min incubation, with a further loss of activity detected at 30 and 60 min, indicating that inhibition occurs in a time-dependent manner (Figure 5). Similar experiments in which 100 mM Cl^- or 100 μM Br^- were used in place of SCN^-, resulted in a loss of PTP activity after 15 min, but no further loss of activity at longer incubation times (Figure 5). At each of the non-zero time points the extent of inhibition induced by the SCN^- system was significantly greater than that observed with the Cl^-

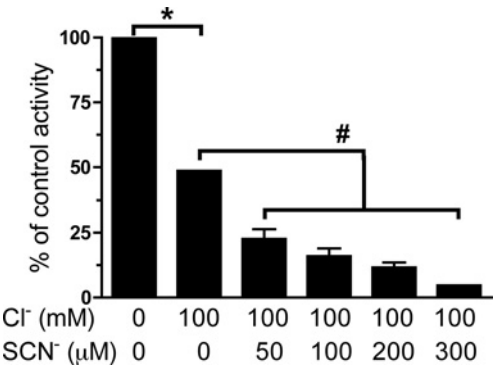

Figure 6 Concentration-dependent inhibition of PTP activity in J774A.1 cell lysates by MPO-derived HOCl and HOSCN

PTP activity in cell lysates (0.33 ± 0.03 mg of cell protein/ml) was determined after incubation with 100 nM MPO, 100 mM Cl^- and increasing concentrations of SCN^- with 25 μM H_2O_2 for 15 min at 22 °C. Control samples contained cell lysates, MPO and H_2O_2 incubated under the same conditions, but in the absence of any added Cl^- or SCN^-. After incubation MPO was removed before quantification of the released *p*-nitrophenolate anion as described in the legend to Figure 5. Values are means ± S.D. of four determinations from two separate experiments. Statistical analyses were carried out using a repeated measures one-way ANOVA with Bonferroni's post-hoc test. $^*P < 0.05$ for the absence of both Cl^- and SCN^- compared with the presence of 100 mM Cl^-. $\#P < 0.05$ for increasing concentrations of SCN^- in the presence of 100 mM Cl^- compared with the absence of SCN^-.

or Br^- systems. The extent of inhibition induced by the latter two systems was not significantly different. These results indicate that PTPs are rapidly inactivated by each of the MPO/H_2O_2/Cl^-, MPO/H_2O_2/Br^- and MPO/H_2O_2/SCN^- systems. However, the MPO/H_2O_2/SCN^- system induces both a time-dependent loss of activity, and a greater overall extent of inhibition with identical oxidant concentrations.

Subsequent experiments examined the effect of different SCN^- concentrations in the presence of 100 mM Cl^-. Increasing SCN^- concentrations (50–300 μM) in the MPO/H_2O_2/Cl^-/SCN^- system induced greater inhibition at 15 min than MPO/H_2O_2/Cl^- alone (Figure 6). These results indicate that the presence and concentration of SCN^- is a key determinant of the extent of PTP inhibition with the complete MPO/H_2O_2/halide/pseudohalide ion systems.

Treatment of J774A.1 cells with HOSCN promotes MAPK protein phosphorylation

As decreased PTP activity may alter the balance between phosphorylated and non-phosphorylated proteins within cells, the extent of protein phosphorylation in native and HOSCN-treated cells was examined, using both phospho-protein arrays and Western blotting. As a previous study has demonstrated that HOSCN reacts with J774A.1 cells (i.e. is consumed) and induces marked apoptosis [18], activation of the MAPK signalling pathway was examined in detail.

Levels of phosphorylated MAPK proteins in J774A.1 cells (1×10^6 cells) treated with either PBS (control) or 50 μM HOSCN in PBS (pH 7.4) for 15 min at 37 °C were detected using a Proteome Profiler™ Human Phospho-MAPK Antibody Array. Oxidant exposure resulted in significant increases in the levels of phosphorylated p38α and ERK2 (MAPK1) (Figure 7A).

These studies were extended by treating J774A.1 cells (1×10^6) with 0–250 μM HOSCN for 15 min before protein extraction and Western blot analysis of total and phosphorylated forms of p38a, MKK3/6 and ERK1/2. Significant increases in the level of phosphorylated p38α were detected with increasing oxidant

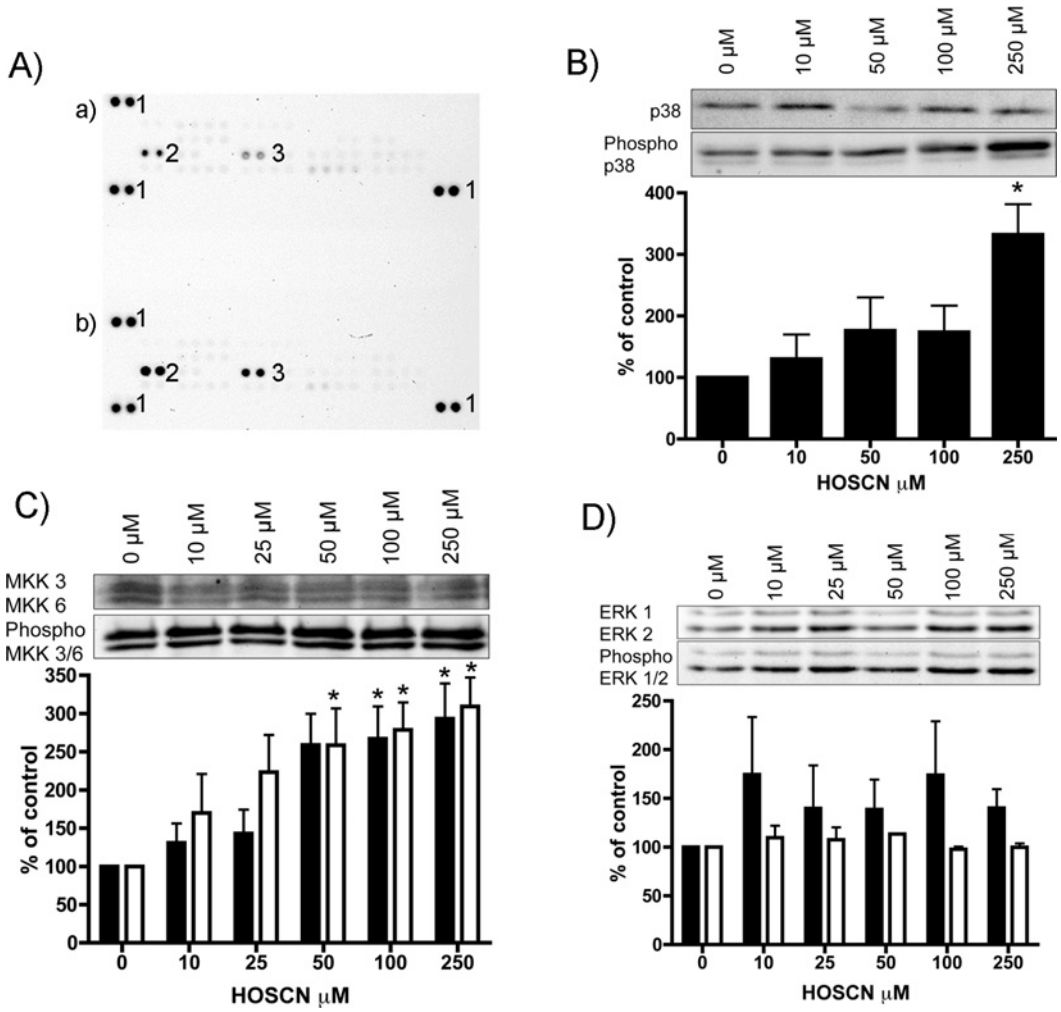

Figure 7 Effect of HOSCN on the extent of protein phosphorylation in J774A.1 cells

(**A**) MAPK array for phosphorylated proteins detected in J774A.1 cells (1×10^6) treated with either (a) PBS or (b) 50 μM HOSCN in PBS, pH 7.4, for 15 min at 37 °C. After oxidant (or control) exposure, cells were lysed using the buffer provided with the kit, and 300 μg of protein (determined using the Bio-Rad protein assay) used for each array. Following binding, the arrays were washed and reacted with the supplied antibody cocktail as specified by the manufacturer. Chemiluminescent detection was performed with ECL with the signals detected using a Bio-Rad ChemiDoc XRS system and Bio-Rad Quantity One software (version 4.6.1). Pairs of protein spots marked '1' are positive controls. Duplicate spots from phosphorylated ERK2 (MAPK1; spots marked '2') and p38α (spots marked '3') are indicated. (**B**) Western blots of total and phosphorylated p38α, and corresponding gel densitometry (ratio of phosphorylated to total, $n = 3$ independent experiments), from cells exposed to HOSCN at the stated concentrations as described for (**A**). (**C**) Western blots of total and phosphorylated MKK3 (solid bars) and MKK6 (open bars), and corresponding gel densitometry (ratio of phosphorylated to total, from three independent experiments), from cells exposed to HOSCN at the stated concentrations as described for (**A**). (**D**) Western blots of total and phosphorylated ERK1 (solid bars) and ERK2 (open bars), and corresponding gel densitometry (ratio of phosphorylated to total, from three independent experiments), from cells exposed to HOSCN at the stated concentrations as described for (**A**). Statistical analyses compared the HOSCN-treated samples with the untreated control (PBS-treated) cells using one-way ANOVA with Bonferroni's post-hoc test, $^*P < 0.05$.

exposure, with no concomitant change in total p38α levels (Figure 7B). Thus the ratio of phosphorylated to total p38α protein was significantly increased with a HOSCN concentration of 250 μM. As p38α phosphorylation is regulated by activated MKK3/6, phosphorylation of this protein complex was also examined. Figure 7(C) shows that there was a dose-dependent increase in phosphorylated MKK3/6 with this being statistically significant at oxidant concentrations $\geqslant$100 μM. Analogous experiments with ERK2 antibodies (native and phosphorylated) did not give rise to a statistically significant increase in the extent of phosphorylation (Figure 7D). The reasons for the discrepancy between these data and those from the Proteome Profiler array (Figure 7A) are unclear.

Levels of the upstream signalling molecules MKK3 and MKK6, their phosphorylated counterparts, and the ratio of these two forms were examined in a similar manner. Both MKK3 and MKK6 showed a dose-dependent increase in the ratio of phosphorylated/non-phosphorylated protein with increasing HOSCN concentrations, with this being significant at 250 and $\geqslant$100 μM HOSCN for MKK3 and MKK6 respectively (Figure 7C).

Activation of the MAPK pathway

The HOSCN-induced increase in MKK3/6 and p38α phosphorylation suggests that this oxidant is activating MAPK signalling. An expected downstream consequence of such activation would be altered transcription of target genes. To test if HOSCN induced differential expression of target genes, J774A.1

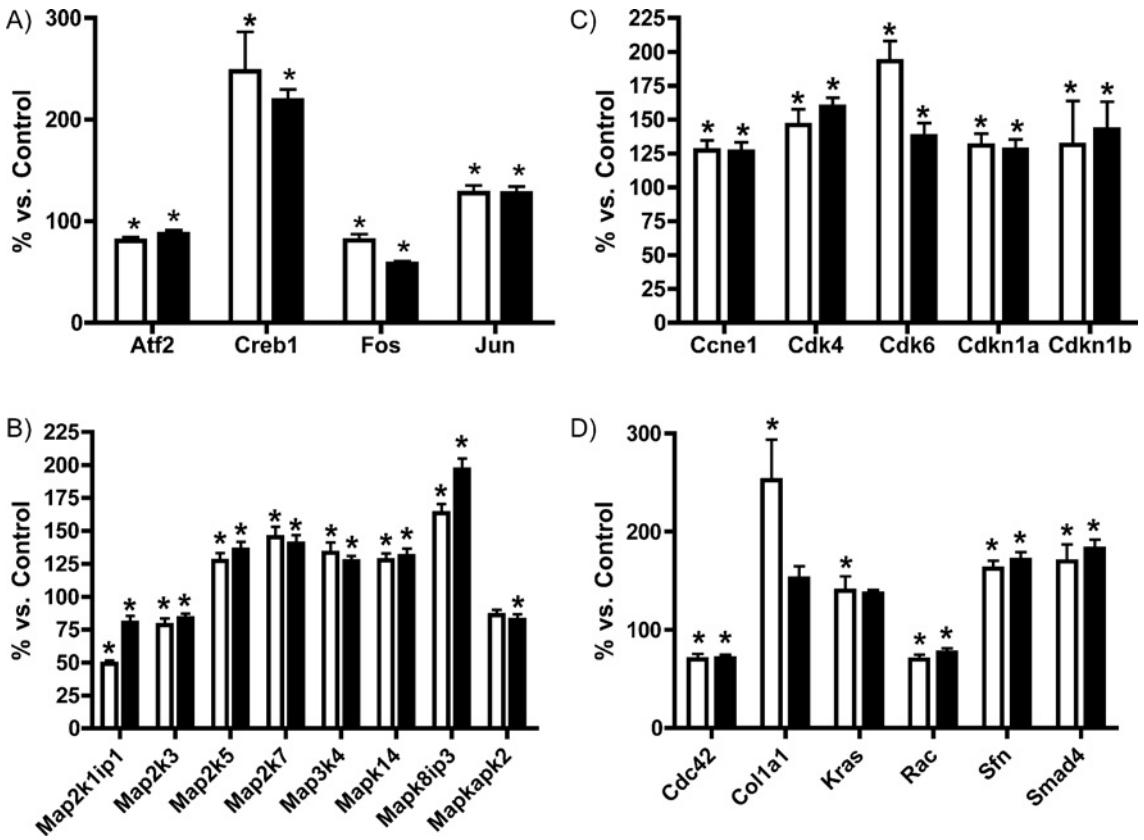

Figure 8 Effect of HOSCN exposure on gene expression in J774A.1 cells

MAPK gene array following treatment of J774A.1 cells with HOSCN. Cells (plated at 0.5×10^6 ml^{-1}) were exposed to 50 μM HOSCN (open bars) or 100 μM HOSCN (solid bars) in PBS at 37 °C for 15 min. Total RNA was subsequently extracted, used to synthesize cDNA and used in the MAPK signalling pathway PCR array as described in the Experimental section. Histograms show data for: (**A**) transcription factors, (**B**) cyclin-related proteins, (**C**) MAPKs and (**D**) other genes. All genes were normalized against five reference genes and data are expressed relative to control (PBS-treated) cells, and are means ± S.E.M. for triplicate determinations from three independent experiments. Statistical analyses compared the HOSCN-treated samples with the no-oxidant (PBS-treated) control cells using one-way ANOVA with Bonferroni's post-hoc test, $^*P < 0.05$.

cells were exposed to 50 or 100 μM HOSCN, then mRNA levels of 84 well-characterized genes associated with MAPK signalling were assayed using a MAPK-specific PCR array. Results show that the mRNA levels of 23 of the 84 genes were significantly altered by HOSCN treatment (Figure 8). These mRNAs encode transcription factors, cyclin-related proteins and MAPK proteins. These changes in mRNA levels confirm that cellular exposure to HOSCN affects the MAPK signalling pathway.

DISCUSSION

MPO, released by activated neutrophils, monocytes and some macrophages, catalyses the oxidation of Cl^-, Br^- and SCN^- by H_2O_2, to HOCl, HOBr and HOSCN respectively (reviewed in [1–3]). These oxidants generated by both MPO [5], and other peroxidases (including salivary, gastric and eosinophil peroxidases; [1]) are important in the innate immune response against invading pathogens [2,3], but have been implicated as damaging agents in multiple human inflammatory pathologies (reviewed in [1–3]). As HOSCN reacts selectively with thiols (both low-molecular-mass and protein-bound [14,15,36]), it was postulated that this oxidant might interfere with cell survival and signalling processes dependent on PTPs, as these enzymes have a conserved, low pK_a, active site cysteine residue.

The results reported in the present paper indicate that both pre-formed HOSCN and a MPO/H_2O_2/SCN^- system can inhibit PTP activity of isolated PTP1B (with concomitant modification of cysteine residues on this protein), in cell lysates, and intact J774A.1 macrophage-like cells. The HOSCN concentrations that induce inhibition are within the concentration ranges believed to be present at sites of inflammation (compared with hundreds of micromolar generated by stimulated neutrophils at the concentration present in blood [3], and millimolar concentrations within the neutrophil phagosome [37]). The levels of SCN^- required to form these concentrations of HOSCN are within those detected in plasma, especially in heavy smokers [9].

PTP inhibition was also detected with MPO/H_2O_2/halide ion systems using typical plasma concentrations of Cl^- (to generate HOCl) and Br^- (to give HOBr) [4], indicating that these oxidants can also modulate PTP activity. Both HOCl and HOBr react more rapidly than HOSCN with cysteine residues (and other species [13,15]), but are less selective in their reactions, consistent with the rapid loss of PTP activity, and the slower, but greater, extent of inhibition seen with HOSCN (compared with HOCl and HOBr) at longer time points. This is ascribed to a rapid and indiscriminate consumption of the HOCl or HOBr by other cellular targets, compared with a slower, but more selective, oxidation of cysteine residues by HOSCN. Cysteine oxidation by HOSCN, although slower than with HOCl and HOBr (k for both oxidants approx. 3×10^7 $M^{-1} \cdot s^{-1}$ [38,39]; compared with 8×10^4 $M^{-1} \cdot s^{-1}$ for HOSCN [15]), is much more rapid than for H_2O_2 (see below) and peroxynitrite (approx. 9×10^3 $M^{-1} \cdot s^{-1}$ [40]).

Inhibition of isolated PTP1B occurred with much lower oxidant concentrations than the loss of PTP activity in cell lysates and intact cells, with this ascribed to the presence of alternative reactive targets in the lysate and intact cell systems. Thus in these more complex systems there are multiple PTP isoforms (the human genome encodes >100 PTPs [22,23]) that will contribute to the overall activity detected. The observed inhibition curves are therefore likely to be composites of the effects on multiple different enzymes, each of which may have a different susceptibility to oxidation. The pattern of inhibition detected with both the lysates and intact cells is consistent with populations that are both highly sensitive to oxidation (as indicated by the rapid partial loss of overall PTP activity with low concentrations of oxidant in Figure 2), and much more resistant (as indicated by the significant non-zero activity at very high oxidant concentrations; Figure 2). This differential susceptibility to oxidation may also rationalize the different oxidant concentrations required to induce changes in the extent of protein phosphorylation detected with p38a compared with MKK3/6.

The PTP inhibition observed in cell lysates could be reversed by DTT at short incubation times. These results are consistent with the initial reaction of the HOSCN with cysteine residues to give a cysteine–SCN adduct (see [17,41]). These adducts can be readily reduced by DTT, regenerating the free thiol. The cysteine–SCN adduct may also undergo subsequent slow hydrolysis to give a sulfenic acid (RSOH) [42,43], an intermediate known to be important in redox signalling and which is also reducible by DTT [44], or further oxidation to give sulfinic (RSO_2H) or sulfonic (RSO_3H) acids (as seen with peroxiredoxins [45]). Sulfinic and sulfonic acids do not appear to be rapidly repaired within cells [44].

This reversible PTP inhibition at early time points indicates that oxidation of protein cysteine residues by HOSCN may serve as a signalling phenomenon. Previous studies have reported that PTPs can be specifically and reversibly inhibited by H_2O_2, and this modulates cell signalling [22,46]. Although this effect is well established, rate constants, k, for the reaction of H_2O_2 with the active site cysteine residues of PTPs have not been determined. Data in the literature indicate that k for the reaction of H_2O_2 with protein cysteine residues varies markedly (from a value of 3 $M^{-1} \cdot s^{-1}$ for Cys^{34} on human serum albumin [47] to approx. 10^7 $M^{-1} \cdot s^{-1}$ for peroxiredoxins [48]). Owing to the low concentrations of purified enzyme available, kinetic data are not available for the reaction of HOSCN with PTPs, but it has been reported that this oxidant reacts with other protein cysteine residues, including the Cys^{34} residue on BSA, with rate constants in the range $1–7 \times 10^4$ $M^{-1} \cdot s^{-1}$ [15]; these reactions are therefore likely to be much more rapid than the corresponding reactions for H_2O_2. The higher rates of reaction of HOSCN over H_2O_2, and the absence of any known detoxifying agent for this oxidant (unlike the situation with H_2O_2, which is rapidly removed by glutathione peroxidases, peroxiredoxins and catalase [49]), suggests that HOSCN may play an important role in modulating cell signalling as a result of its much greater rate of reaction, and hence potentially greater and more rapid effect at low concentrations. However, it should be noted that HOSCN also reacts much more rapidly with the important cellular antioxidant GSH, which will be a competing target within cells, than H_2O_2 (k $2.5–8 \times 10^4$ $M^{-1} \cdot s^{-1}$ [15,16] compared with 0.87 $M^{-1} \cdot s^{-1}$ for HOSCN and H_2O_2 respectively at pH 7.4 [50]), so the significance of the greater reactivity of HOSCN is less clear.

The results of the present study indicate that a major functional consequence of PTP inhibition is hyperphosphorylation of some important cellular signalling proteins, thereby providing a novel mechanism by which MPO-derived HOSCN can modulate cell signalling and survival events. This inhibition of PTP activity has potential major ramifications for signalling pathways {e.g. those involving NF-κB (nuclear factor κB); [24]} dependent on these events, and provides a direct link between thiol oxidation and signalling events involving protein phosphorylation. Increased phosphorylation of p38α, MKK3/6 and (to a lesser extent) ERK1/2 has been detected in cells exposed to HOSCN, with this associated with altered expression of multiple MAPK target genes (including Map2k5, Map2k7, Map3k4, Mapk14 and Mapk8ip3), the transcription factors CREB1 (cAMP-response-element-binding protein 1) and Jun, and a number of cyclin-related proteins. This differential gene expression profile is consistent with an associated activated stress response in the oxidant-exposed cells, culminating in arrest of cell division and induction of apoptosis. In previous studies we have shown that HOSCN induces apoptosis, and to a lesser extent, necrosis [18].

In conclusion, HOSCN formation inhibits PTP activity that in turn affects MAPK signalling. These effects are detected with oxidant levels within the range expected at sites of inflammation, implicating HOSCN-mediated thiol oxidation as an important mediator of inflammation-induced modulation of cellular signalling and oxidative damage. These events may be of significance in both smokers and non-smokers. Smokers have elevated levels of plasma SCN^- that is the precursor of HOSCN, whereas non-smokers can have significant SCN^-levels as a result of biogenesis from alkaloid and cyanogenic materials. Our findings are consistent with elevated SCN^- contributing to an enhanced risk of developing pathologies associated with multiple inflammatory diseases.

AUTHOR CONTRIBUTION

Amanda Lane performed most of the research, analysed the data and contributed to the manuscript preparation. Joanne Tan performed the array experiments and helped analyse the data. Clare Hawkins helped analyse the data, and contributed to the experimental design and writing of the manuscript. Alison Heather assisted with the data analysis and experimental design, and contributed to the manuscript preparation. Michael Davies designed the research and experimental plan, contributed to the manuscript preparation and directed the project.

ACKNOWLEDGEMENTS

The authors thank Dr Philip Morgan and Dr Mitchell Lloyd (The Heart Research Institute) for helpful discussions.

FUNDING

This work was supported by the Australian Research Council under the ARC Centres of Excellence [grant number CE0561607] and Discovery [grant number DP0988311] programmes; and a National Heart Foundation Grant in Aid [grant number G053038].

REFERENCES

1 Davies, M. J., Hawkins, C. L., Pattison, D. I. and Rees, M. D. (2008) Mammalian heme peroxidases: from molecular mechanisms to health implications. Antioxid. Redox Signaling **10**, 1199–1234
2 Klebanoff, S. J. (2005) Myeloperoxidase: friend and foe. J. Leukocyte Biol. **77**, 598–625
3 Kettle, A. J. and Winterbourn, C. C. (1997) Myeloperoxidase: a key regulator of neutrophil oxidant production. Redox Rep. **3**, 3–15
4 Lentner, C. (1984) Geigy Scientific Tables: Physical Chemistry, Composition of Blood, Hematology, Somatometric Data, Ciba-Geigy Ltd, Basle
5 van Dalen, C. J., Whitehouse, M. W., Winterbourn, C. C. and Kettle, A. J. (1997) Thiocyanate and chloride as competing substrates for myeloperoxidase. Biochem. J. **327**, 487–492

6 Hawkins, C. L. (2009) The role of hypothiocyanous acid (HOSCN) in biological systems. Free Radical Res. **43**, 1147–1158
7 Das, D., De, P. K. and Banerjee, R. K. (1995) Thiocyanate, a plausible physiological electron donor of gastric peroxidase. Biochem. J. **305**, 59–64
8 Ihalin, R., Loimaranta, V. and Tenovuo, J. (2006) Origin, structure, and biological activities of peroxidases in human saliva. Arch. Biochem. Biophys. **445**, 261–268
9 Wang, Z., Nicholls, S. J., Rodriguez, E. R., Kummu, O., Horkko, S., Barnard, J., Reynolds, W. F., Topol, E. J., DiDonato, J. A. and Hazen, S. L. (2007) Protein carbamylation links inflammation, smoking, uremia and atherogenesis. Nat. Med. **13**, 1176–1184
10 Ashby, M. T., Carlson, A. C. and Scott, M. J. (2004) Redox buffering of hypochlorous acid by thiocyanate in physiologic fluids. J. Am. Chem. Soc. **126**, 15976–15977
11 Nagy, P., Beal, J. L. and Ashby, M. T. (2006) Thiocyanate is an efficient endogenous scavenger of the phagocytic killing agent hypobromous acid. Chem. Res. Toxicol. **19**, 587–593
12 van der Veen, B. S., de Winther, M. P., Heeringa, P., Augusto, O., Chen, J. W., Davies, M., Ma, X. L., Malle, E., Pignatelli, P. and Rudolph, T. (2009) Myeloperoxidase: molecular mechanisms of action and their relevance to human health and disease. Antioxid. Redox Signaling **11**, 2899–2937
13 Pattison, D. I. and Davies, M. J. (2006) Reactions of myeloperoxidase-derived oxidants with biological substrates: gaining insight into human inflammatory diseases. Curr. Med. Chem. **13**, 3271–3290
14 Arlandson, M., Decker, T., Roongta, V. A., Bonilla, L., Mayo, K. H., MacPherson, J. C., Hazen, S. L. and Slungaard, A. (2001) Eosinophil peroxidase oxidation of thiocyanate. Characterization of major reaction products and a potential sulfhydryl-targeted cytotoxicity system. J. Biol. Chem. **276**, 215–224.
15 Skaff, O., Pattison, D. I. and Davies, M. J. (2009) Hypothiocyanous acid reactivity with low-molecular-mass and protein thiols: absolute rate constants and assessment of biological relevance. Biochem. J. **422**, 111–117
16 Nagy, P., Jameson, G. N. and Winterbourn, C. C. (2009) Kinetics and mechanisms of the reaction of hypothiocyanous acid with 5-thio-2-nitrobenzoic acid and reduced glutathione. Chem. Res. Toxicol. **22**, 1833–1840
17 Hawkins, C. L., Pattison, D. I., Stanley, N. R. and Davies, M. J. (2008) Tryptophan residues are targets in hypothiocyanous acid-mediated protein oxidation. Biochem. J. **414**, 271–280
18 Lloyd, M. M., van Reyk, D. M., Davies, M. J. and Hawkins, C. L. (2008) Hypothiocyanous acid is a more potent inducer of apoptosis and protein thiol depletion in murine macrophage cells than hypochlorous acid or hypobromous acid. Biochem. J. **414**, 271–280
19 Botti, T. P., Amin, H., Hiltscher, L. and Wissler, R. W. (1996) A comparison of the quantitation of macrophage foam cell populations and the extent of apolipoprotein E deposition in developing atherosclerotic lesions in young people: high and low serum thiocyanate groups as an indication of smoking. Atherosclerosis **124**, 191–202
20 Scanlon, C. E. O., Berger, B., Malcom, G. and Wissler, R. W. (1996) Evidence for more extensive deposits of epitopes of oxidized low density lipoproteins in aortas of young people with elevated serum thiocyanate levels. Atherosclerosis **121**, 23–33
21 Sirpal, S. (2009) Myeloperoxidase-mediated lipoprotein carbamylation as a mechanistic pathway for atherosclerotic vascular disease. Clin. Sci. **116**, 681–695
22 Chiarugi, P. and Buricchi, F. (2007) Protein tyrosine phosphorylation and reversible oxidation: two cross-talking posttranslation modifications. Antioxid. Redox Signaling **9**, 1–24
23 den Hertog, J., Ostman, A. and Bohmer, F. D. (2008) Protein tyrosine phosphatases: regulatory mechanisms. FEBS J. **275**, 831–847
24 Jung, K. J., Lee, E. K., Yu, B. P. and Chung, H. Y. (2009) Significance of protein tyrosine kinase/protein tyrosine phosphatase balance in the regulation of NF-κB signaling in the inflammatory process and aging. Free Radical Biol. Med. **47**, 983–991
25 Chiarugi, P. (2005) PTPs versus PTKs: the redox side of the coin. Free Radical Res. **39**, 353–364
26 Sullivan, S. G., Chiu, D. T., Errasfa, M., Wang, J. M., Qi, J. S. and Stern, A. (1994) Effects of H_2O_2 on protein tyrosine phosphatase activity in HER14 cells. Free Radical Biol. Med. **16**, 399–403
27 Takakura, K., Beckman, J. S., MacMillan-Crow, L. A. and Crow, J. P. (1999) Rapid and irreversible inactivation of protein tyrosine phosphatases PTP1B, CD45, and LAR by peroxynitrite. Arch. Biochem. Biophys. **369**, 197–207
28 von Montfort, C., Sharov, V. S., Metzger, S., Schoneich, C., Sies, H. and Klotz, L. O. (2006) Singlet oxygen inactivates protein tyrosine phosphatase-1B by oxidation of the active site cysteine. Biol. Chem. **387**, 1399–1404
29 Gracanin, M. and Davies, M. J. (2007) Inhibition of protein tyrosine phosphatases by amino acid, peptide and protein hydroperoxides: potential modulation of cell signaling by protein oxidation products. Free Radical Biol. Med. **42**, 1543–1551
30 Stoker, A. W. (2005) Protein tyrosine phosphatases and signalling. J. Endocrinol. **185**, 19–33
31 van Montfort, R. L., Congreve, M., Tisi, D., Carr, R. and Jhoti, H. (2003) Oxidation state of the active-site cysteine in protein tyrosine phosphatase 1B. Nature **423**, 773–777
32 Weibrecht, I., Bohmer, S. A., Dagnell, M., Kappert, K., Ostman, A. and Bohmer, F. D. (2007) Oxidation sensitivity of the catalytic cysteine of the protein-tyrosine phosphatases SHP-1 and SHP-2. Free Radical Biol. Med. **43**, 100–110
33 Furtmuller, P. G., Jantschko, W., Regelsberger, G., Jakopitsch, C., Arnhold, J. and Obinger, C. (2002) Reaction of lactoperoxidase compound I with halides and thiocyanate. Biochemistry **41**, 11895–11900
34 Nelson, D. P. and Kiesow, L. A. (1972) Enthalpy of decomposition of hydrogen peroxide by catalase at 25 °C (with molar extinction coefficients of H_2O_2 solutions in the UV). Anal. Biochem. **49**, 474–478
35 Dremina, E. S., Sharov, V. S., Davies, M. J. and Schoneich, C. (2007) Oxidation and inactivation of SERCA by selective reaction of cysteine residues with amino acid peroxides. Chem. Res. Toxicol. **20**, 1462–1469
36 Nagy, P. and Ashby, M. T. (2005) Reactive sulfur species: kinetics and mechanism of the oxidation of cystine by hypochlorous acid to give N,N′-dichlorocystine. Chem. Res. Toxicol. **18**, 919–923
37 Winterbourn, C. C., Hampton, M. B., Livesey, J. H. and Kettle, A. J. (2006) Modeling the reactions of superoxide and myeloperoxidase in the neutrophil phagosome: implications for microbial killing. J. Biol. Chem. **281**, 39860–39869
38 Pattison, D. I. and Davies, M. J. (2001) Absolute rate constants for the reaction of hypochlorous acid with protein side chains and peptide bonds. Chem. Res. Toxicol. **14**, 1453–1464
39 Pattison, D. I. and Davies, M. J. (2004) A kinetic analysis of the reactions of hypobromous acid with protein components: implications for cellular damage and the use of 3-bromotyrosine as a marker of oxidative stress. Biochemistry **43**, 4799–4809
40 Alvarez, B., Ferrer-Sueta, G., Freeman, B. A. and Radi, R. (1999) Kinetics of peroxynitrite reaction with amino acids and human serum albumin. J. Biol. Chem. **274**, 842–848
41 Aune, T. M., Thomas, E. L. and Morrison, M. (1977) Lactoperoxidase-catalyzed incorporation of thiocyanate ion into a protein substrate. Biochemistry **16**, 4611–4615
42 Aune, T. M. and Thomas, E. L. (1978) Oxidation of protein sulfhydryls by products of peroxidase-catalyzed oxidation of thiocyanate ion. Biochemistry **17**, 1005–1010
43 Nagy, P., Lemma, K. and Ashby, M. T. (2007) Reactive sulfur species: kinetics and mechanisms of the reaction of cysteine thiosulfinate ester with cysteine to give cysteine sulfenic acid. J. Org. Chem. **72**, 8838–8846
44 Poole, L. B., Karplus, P. A. and Claiborne, A. (2004) Protein sulfenic acids in redox signaling. Annu. Rev. Pharmacol. Toxicol. **44**, 325–347
45 Lim, J. C., Choi, H. I., Park, Y. S., Nam, H. W., Woo, H. A., Kwon, K. S., Kim, Y. S., Rhee, S. G., Kim, K. and Chae, H. Z. (2008) Irreversible oxidation of the active-site cysteine of peroxiredoxin to cysteine sulfonic acid for enhanced molecular chaperone activity. J. Biol. Chem. **283**, 28873–28880
46 Denu, J. M. and Tanner, K. G. (1998) Specific and reversible inactivation of protein tyrosine phosphatases by hydrogen peroxide: evidence for a sulfenic acid intermediate and implications for redox regulation. Biochemistry **37**, 5633–5642
47 Turell, L., Botti, H., Carballal, S., Ferrer-Sueta, G., Souza, J. M., Duran, R., Freeman, B. A., Radi, R. and Alvarez, B. (2008) Reactivity of sulfenic acid in human serum albumin. Biochemistry **47**, 358–367
48 Ogusucu, R., Rettori, D., Munhoz, D. C., Netto, L. E. and Augusto, O. (2007) Reactions of yeast thioredoxin peroxidases I and II with hydrogen peroxide and peroxynitrite: rate constants by competitive kinetics. Free Radical Biol. Med. **42**, 326–334
49 Halliwell, B. and Gutteridge, J. M. C. (2007) Free Radicals in Biology and Medicine, Oxford University Press, Oxford
50 Winterbourn, C. C. and Metodiewa, D. (1999) Reactivity of biologically important thiol compounds with superoxide and hydrogen peroxide. Free Radical Biol. Med. **27**, 322–328

Received 12 January 2010/8 June 2010; accepted 9 June 2010
Published as BJ Immediate Publication 9 June 2010, doi:10.1042/BJ20100082